BioGecko
Vol 12 Issue 02 2023
ISSN NO: 2230-5807

State of Charge Estimation of Li-ion Battery Using Unscented Kalman Filter

Sonu Kumar[1], S. Koteswara Rao[2]

[1]Post Doctoral Research Fellow, Department of Electronics and Communication Engineering, Koneru Lakshmaiah Education Foundation, Vaddeswaram, Guntur, Andhra Pradesh-522502, India

[2]Professor, Department of Electronics and Communication Engineering, Koneru Lakshmaiah Education Foundation, Vaddeswaram, Guntur, Andhra Pradesh-522502, India

Abstract
An essential indicator for Li-ion batteries is their state of charge (SOC). The safe operation of a Li-ion battery can be ensured by an accurate SOC estimation. A precise estimation of the remaining energy level or SOC of the cell or battery pack is necessary for battery management systems (BMS). However, in an operational environment with Gaussian noise, the conventional estimation approach, has a cumulative inaccuracy and is unable to sustain satisfactory results for an extended period of time. The estimation error brought on by Gaussian noise can be eliminated using the Kalman filtering process.For the purpose of estimating the state of charge, three Kalman filters, Extended Kalman Kalman filters (EKF), Adaptive Extended Kalman filters (AEKF) andUnscented Kalman filters (UKF) were created and studied. The test system is created in MATLAB/Simulink to examine the effectiveness of the various approaches. Different models are developed and tested.Simulation findings demonstrate that the suggested UKF based method outperforms conventional methods and has a higher estimation accuracy under various operating conditions.A comparison between EKF, AEKF and UKF shows UKF gives minimum SOC estimation error within the range of 0.10%.

Keywords: Battery; SOC Estimation; Kalman filters; UKF; Dynamic modelling; battery management system

1. Introduction

Two major issues facing the world in recent years are environmental pollution and the energy crisis [1]. The sharp rise in the number of fossil fuel vehicles makes these issues worse. Sustainable development places a strong emphasis on the replacement of fossil fuels with low-carbon and effective energy sources. Energy Storage is a crucial component in producing renewable energy, and Li-ion batteries are the most popular option due to a number of benefits, including comparably better charge and discharge performance, high energy and charge densities.Due to its high energy density, extended cycle life, and rapid charging time, lithium-ion batteries are frequently used in smart home applications [2]. Li-ion batteries play a vital role in the advancement of modern technology, such as electric vehicles (EVs), because to their attributes of long cycle life, high power endurance and high power density [3-5]. The battery's capacity is reflected by the state of charge (SOC), which is a crucial indicator. The battery management system's ability to accurately estimate SOC during the charge and discharge is crucial.

Precise SOC calculation takes into account important data including battery performance and remaining life [6], which in turn helps to manage and use battery power and energy [7] more effectively. Additionally, over-discharging and over-charging of the battery, which shorten battery life, cause explosions or flames, accelerate ageing and permanently harm the cell structure of batteries, which can be controlled using proper SOC estimation [8].The Battery Management System (BMS), which controls the energy flow in a battery pack with respect to individual cell voltages, temperature, state of charge, and condition of health, is typically programmed with the SOC estimation algorithm. The primary purpose of BMS is to keep the battery system's operating environment secure and to guard against damage [9]. Although the calculation of battery SOC is a crucial BMS function, the non-linear, intricate electrochemical process in the battery makes it difficult to estimate accurately online [10].

Many studies have used different techniques to estimate SOC in recent years, including the amperehour integration approach (Ah) [11], the Kalman filter method (KF) [12–14], and deep reinforcement learning (DRL) [15–18]. The Ah is used the most frequently among them. The outdated techniques for determining the SOC include counting Ah and measuring impedance. The SoC can be determined via Ah counting as given below [19]:

$$SoC(t) = SoC(t_0) + \int_{t_0}^{t} \frac{\eta I_t}{3600 C_0} d\tau \quad (1)$$

where SoC(t_0), C_0, h, and I_t indicate the battery's starting SOC, maximum capacity, coulomb factor, and terminal current.

Ah approach, however, has a cumulative inaccuracy and is unable to fix the divergence of the starting value of SOC [20]. The accuracy decreases over time. The Ah counting method is regarded as imprecise since the current measurement inaccuracy accumulates. Moreover, it is unable to determine the SoC's starting value. The second method [21–22] uses the open-circuit voltage (OCV) to calculate SoC in accordance with the battery's OCV–SoC curve.

The most frequent methods for SOC estimation utilized include: coulomb counting, open circuit voltage (OCV) estimation, electrochemical impedance spectroscopy (EIS), and filtering. Some of the most commonly used SOC estimation methods are listed in Table 1. However, the OCV is measured after the battery has been removed from the circuit, hence this method is unable to identify the SoC when it is operating continuously. Due to the fact that battery impedance varies with SoC, the SoC can also be inferred from battery impedance. However, because battery impedance is temperature dependent, additional tools are required to measure it.

Table 1: Different SOC Estimation Methods

Category	Methods
Direct Measurement	Open circuit voltage, Terminal voltage, Impedance method
Book keeping method	Coulomb counting, Modified coulomb counting
Indirect measurement	Neural network, support vector, fuzzy logic, Kalman filter, Extended Kalman filter, Unscented Kalman filter, Cubature Kalman filter, Particle filter, H infinity filter, Nonlinear observer, Sliding mode observer, Proportional integralobserver
Hybrid methods	Coulomb counting and Kalman filter, Kalman filter and Long short-termmemory

Recently, SOC has been estimated using a variety of adaptive techniques, such as fuzzy logic, neural networks, adaptive observers, and Kalman filters [23]. Other techniques for SoC estimation include robust and adaptive observers [24,25]. For a linear or piecewise linear battery model, robust H∞ observers can be created to estimate the SoC [26]. An H∞ observer taking into account an electrochemical impedance model for SoC estimate is introduced by Chen et al. [27]. However, the robust-observer approach cannot be used in low-cost microelectromechanical (MEMS) devices because the H∞ algorithm requires extensive matrix operations.

For SoC estimation, adaptive model reference observer [28], particle filter [29] and nonlinear approaches [30] are also used. Hu et al. [31] provided a technique for estimating SoC taking into account the time-varying model parameters taking into account temperature variations during the tests. Nevertheless, determining model parameters for various temperature ranges takes time and is expensive.

Another nonlinear technique for SoC estimation is sliding-mode observer (SMO). This observer takes the battery's nonlinear model with uncertainties into account [32, 33]. The chattering phenomenon is the SMO-based approaches' fundamental flaw. These observers have strong robustness because they can deal with the ambiguity in the model parameters. In order to minimize chattering, Chen et al. [34] introduce an adaptive switching-gain SMO for SoC estimation. The strategy is challenging to put into practise, though.

Another group of SoC estimate techniques is intelligence-based techniques, which includes neural networks, fuzzy neural networks, and fuzzy adaptive neural networks [35–39]. These techniques have various drawbacks. Although the neural network-based approaches do not require a mathematical model of the batteries, complete and trustworthy datasets are required for training, testing and validation. Inaccurate SoC estimation can also result from using the same training dataset for batteries of varied ages [40]. Additionally, this method's implementation on the CPU presents its own challenges. The fuzzy inference systems also rely on the expertise of experts [41]. Problems arise while choosing the membership functions for the fuzzy system design due to expert disagreements. There are also learning-based options for the SoC estimation, including deep learning [42] and machine learning [43]. The distribution of the training data and test data is assumed to be the same by the deep-learning algorithms for the SoC estimate. But in reality, this presumption is incorrect. A deep-transfer neural network with multiscale distribution adaptation was given in [44] for the SoC estimate as a solution to this issue, but the main disadvantage of this approach was its difficult implementation. Since they do not require the dynamic model of the battery, learning-based approaches are often good for SoC estimate. However, a sizable, trustworthy training dataset is needed for these techniques. Additionally, they need the distribution of the training and test data as well as pricey graphics processing units (GPU).

Rudolph Kalman [45] created one of the most used algorithms, the KF, in 1960. It was initially used to predict the trajectories of both manned and unmanned spacecraft. The Kalman filter, a recursive algorithm for estimating state variables of a dynamic system, has been used to predict battery SoC. Despite the measurement noise, this optimal observer can offer a precise evaluation of the states. Among these techniques, the Kalman filtering seems to be very promising [46]. Plett [47–49] presented a technique in 2004 for using the KF to estimate the SOC of LICs, which is not observable directly. This approach was frequently modified in later works, leading to a variety of KF-based state estimation implementations. In real-world applications, it filters the system's input and output signals to precisely forecast the dynamic state of the system. The interference brought on by white noise in the system can be eliminated by the extended Kalman filter (EKF) approach, and the cumulative error brought on by the ampere-time integration method can be reduced.

As the battery model is nonlinear, the SoC is commonly estimated using the extended Kalman filter (EKF) [50–53]. Additionally, the lifetime of lithium-ion batteries has changed their electrochemical characteristics, which can cause the EKF method to estimate SoC and SoH incorrectly. KFs have the advantage of taking model and measurement errors into account, which produces a robust estimating behaviour. A cell depends on SOC, temperature, current and age [54], and because a model cannot account for every scenario, its uncertainties change as it operates.

In [55], an adaptive extended Kalman filter (AEKF), which employs a covariance adaptation technique, is presented to enhance the performance of the Kalman filter in SoC estimation. The estimation algorithm's linearization inaccuracy is this filter's fundamental flaw. In [56,57], the unscented Kalman filter (UKF) and adaptive UKF are used to address this issue. Additionally [41], implements a sigma-point EKF on the battery model. Recently, an interactive multi-model UKF [59] and a central-difference Kalman filter (CDKF) were also constructed for SoC estimation. These solutions, however do not account for model uncertainties and rely heavily on precise battery models.

However, the main drawbacks of the existing approaches can be summed up as (a) the traditional observers, like SMO and H∞, have chattering in their response or require complicated mathematical calculation and not able to estimate SOC when measurements noise are present, (b) the artificial intelligence-based approaches require a trustworthy training dataset or specialists' knowledge of the battery; (c) KF based approaches depends on precise battery models and not able to estimate SOC properly when model uncertainties are present. A detailed description about the advantages and disadvantages different SOC estimation methods are listed in Table 2.

Table 2. Merits and demerits of various SoC estimation techniques

Technique	Advantages	Disadvantages
Ampere-hour (Ah) counting approach	Less calculation, low cost, and easy implementation	Error accumulates
Impedance measurement approach	Low calculation, low cost, and easy implementation	Sensitive to temperature change and time-taking process
AI (Deep learning and Machine learning) algorithm	Battery model not required	Large and accurate training data is necessary, and both training and test data must be distributed, costly GPU
Kalman filters-based approach	Can estimate while measurement and process noises are present	Battery model accuracy is required, as well as knowledge of measurement and process noises.
H∞ observer	SoC estimation without knowledge of the statistical properties of the battery	Heavy processors are required for calculation.
Sliding mode-based observers	Tolerance to uncertainties in the model	Chattering occurrences and slow convergence

This study offers an UKF based SOC estimation utilising an equivalent battery circuit model. The equivalent circuit model demonstrates the nonlinear relationship between the OCV and SOC by including capacitors, resistors and a nonlinear voltage source. The battery models are described in the below section.

2. Battery SOC Estimation Model

For use in several applications, electrochemical batteries come in a variety of models. The electro-circuit model is suitable for the implementation of estimate algorithms like SoC or SoH estimation. These models can be categorised into electrochemical, electro-circuit and intelligent models. The Rint model [60], Thevenin model [61], and Rngv model [62] are three common Li-ion battery related models. Among these, the Thevenin model can instantly represent the Li-ion battery's operational condition without adding too much delay to track the actual voltage, ensuring the model's correctness over the course of a lengthy simulation. Fig. 1 depicts the Thevenin model's structural layout.

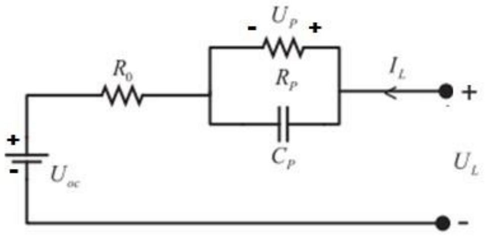

Fig. 1. Thevenin equivalent circuit model

The circuit equations for Thevenin's model are given below using Kirchhoff's Voltage Law and Kirchhoff's Current Law as reference.

$$\dot{U}_P = -\frac{U_P}{R_P C_P} + \frac{I_L}{C_P}$$
$$U_L = U_P + U_{OC} + I_L R_0 \tag{2}$$

where I_L is the current through the resistance R_0, U_L is terminal voltage for analogous circuit, U_P is the terminal voltage for the polarization capacitor C_P, U_{OC} is open circuit voltage of equivalent circuit.

The concept of Ah is used to describe the value of SOC, and the resulting equation is illustrated below.

$$SOC(t) = SOC(t_0) + \frac{\int_{t_0}^{t} k_T i(\tau) d\tau}{Q_N} \tag{3}$$

where $SOC\ (t_0)$ is the SOC of Li-ion battery at moment t_0, k_T is Li-ion battery's temperature correction factor at temperature $T, i\ (\tau)$ is battery's current at instant τ, and Q_N is its rated capacity.

Calculating the battery's open circuit voltage will yield the SOC. This method's SOC estimate equation is provided below.

$$SOC(t) = SOC(OCV) + \frac{\int_{t_0}^{t} k_T i(\tau) d\tau}{Q_N} \tag{4}$$

where OCV is the open circuit voltage value, SOC (OCV) is the matching SOC's starting value. The discrete state space model of this estimating method is depicted below when combined (3) with the Thevenin model.

$$\begin{bmatrix} SOC_k \\ U_{P,k} \end{bmatrix} = \begin{bmatrix} 1 & 0 \\ 0 & e^{-\frac{\Delta T}{R_P C_P}} \end{bmatrix} \begin{bmatrix} SOC_{k-1} \\ U_{P,k-1} \end{bmatrix} + \begin{bmatrix} \frac{\Delta T}{Q_N} \\ \left(1 - e^{-\frac{\Delta T}{R_P C_P}}\right) R_P \end{bmatrix} I_{k-1} + w_{k-1} \tag{5}$$

$$U_{L,k} = OCV\ (SOC_k) + U_{P,k} + R_0 I_k + v_k \tag{6}$$

where ΔT is the discrete step size, w_{k-1}denotes process noise at instant k -1, v_k denotes observed noise at instant k.

This nonlinear estimating issue can be resolved using the EKF technique. It uses a recursive technique to accomplish minimum variance estimation and can provide the estimate's error. This algorithm is an optimal autoregressive data processing algorithm. The discrete nonlinear state space model is given below.

$$\begin{cases} x_k = f(x_{k-1}, u_{k-1}, w_{k-1}) \\ y_k = h(x_k, u_k, v_k) \end{cases}$$
$$w_k \sim (0, Q)$$
$$v_k \sim (0, R) \tag{7}$$

Process noise at instant k-1 is denoted by w_{k-1}, measurement noise at instant k is denoted by vk, covariance of wk and vk are denoted by Q and R, respectively.

The system is linearized at an operating point to convert a nonlinear problem into a linear one. At this moment, the state equation is converted into the Taylor expansion at $x_{k-1} = x_{k-1}|k\text{-}1$, $w_{k-1} = 0$.

$$\widetilde{w}_k \sim \left(0, L_k Q L_k^T\right) \tag{8}$$
$$\tilde{v}_k \sim \left(0, M_k R M_k^T\right) \tag{9}$$

The EKF method must estimate the P_k and x_k in two separate ways during each sample cycle, including priori estimation and posteriori estimation. The priori estimate is used to determine the Kalman gain coefficient K_k between the two phases.

The robust-CDKF approach [63] that has been suggested uses the electrical model that is illustrated in Figure 2. Electrochemical models, experimental models, electrical models, abstract models based on artificial intelligence and more models exist for electrochemical batteries. Thevenin models, Impedance models, Runtime based models and Randle equivalent-circuit models are only a few of the several types of electrical models. All of the battery's dynamic properties, such as the non-linear OCV, current, temperature,

BioGecko Vol 12 Issue 02 2023

ISSN NO: 2230-5807

number of cycles, time-dependent storage capacity and transient responses are included in this model.According to the Kirchhoff laws, the terminal voltage can be written as follows.

$$V_t = V_{oc}(SOC) - V_1 - V_2 - I_t R_{in} \tag{10}$$

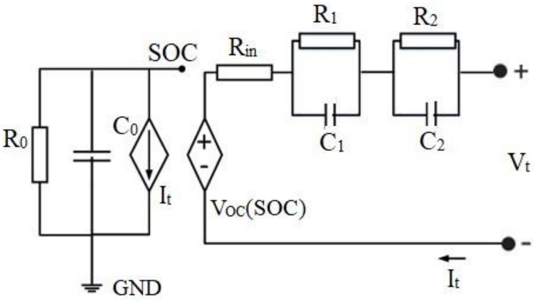

Fig. 2. The battery model

The dynamics of the state of charge and polarization voltages are as follows:

$$\dot{SOC} = -\frac{1}{R_0 C_0} SOC - \left(\frac{I_t}{C_0}\right) + \Delta f_1 \tag{11}$$

$$\dot{V}_2 = -\frac{V_2}{R_2 C_2} + \frac{I_t}{C_2} + \Delta f_3 \tag{12}$$

Where voltages V_1 and V_2 are corresponds to the electrochemical and concentrate respectively. Uncertainties in the battery model and the internal/external disturbances are included in Δf_1 to Δf_3. The updated mean covariance matrix and updated mean estimation of the battery's state variables, as well as the SoC are determined in the last phase.

$$\hat{X}_i = \hat{X}_{i|i-1} + K_i\left(Y_i - \hat{Y}_i\right) \tag{13}$$

$$\hat{P}_i = \hat{P}_{i|i-1} - K_i \hat{P}_y K_i^T \tag{14}$$

Varying-parameter model

It is preferred to include the battery's hysteresis as an additional system state. The discussed issues with the zero-state model are resolved by adding SOC to the state vector to augment the hysteresis and by utilising a Kalman filtering approach to estimate both OCV and SOC. The hysteresis-state model developed by Plett [64] is applied in this work using the following formulation:

$$\frac{dh(SOC,t)}{dSOC} = \gamma sgn(\dot{SOC})(M\left(SOC, \dot{SOC}) - h(SOC,t)\right) \tag{15}$$

The maximum polarisation brought on by battery hysteresis as a result of SOC and its rate of change is known as $M\left(SOC, \dot{SOC}\right)$.

The model yield output can be represented considering hysteresis.

$$V_k = \text{OCV}(SOC_k) - Ri_k + h_k \tag{16}$$

Extended Kalman filtering for zero-state hysteresis model [64] is summarized below.

Nonlinear state-space model

$$SOC_{k+1} = SOC_k - \frac{\eta_i i_k \Delta t}{C_n} + w_k \tag{17}$$

$$V_k = \text{OCV}(SOC_k) - Ri_k - s_k M + v_k \tag{18}$$

Where w_k is independent zero-mean, gaussian noises with covariance P_v

v_k is independent zero-mean, gaussian noises with covariance P_w

$$\dot{C}_k = \frac{\partial \text{OCV}(SOC_k)}{\partial SOC_k}|_{SOC_k = \dot{SOC}_k^-} \tag{19}$$

Initializing k=0,

$$SOC_0^+ = E[SOC_0] \tag{20}$$

$$P^{+}_{\widehat{SOC},0} = \mathrm{E}\,[(SOC_0 - \widehat{SOC}_0^{+})(SOC_0 - \widehat{SOC}_0^{+})^T] \tag{21}$$

Computing k=1, 2, …..

$$\widehat{SOC}_k^{-} = \widehat{SOC}_{k-1}^{+} - \frac{\eta_i i_{k-1}\Delta t}{C_n} \tag{22}$$

$$P^{-}_{\widehat{SOC},k} = P^{+}_{\widehat{SOC},k-1} + P_w \tag{23}$$

Update on measurements

$$L_k = P^{-}_{\widehat{SOC},k}\hat{C}_k^T[\hat{C}_k P^{-}_{\widehat{SOC},k}\hat{C}_k^T + P_v]^{-1} \tag{24}$$

$$\widehat{SOC}_k^{+} = \widehat{SOC}_k^{-} + L_k[V_k - OCV(SOC_k) + Ri_k + s_k M] \tag{25}$$

$$P^{+}_{\widehat{SOC},k} = (1 - L_k\hat{C}_k)P^{-}_{\widehat{SOC},k} \tag{26}$$

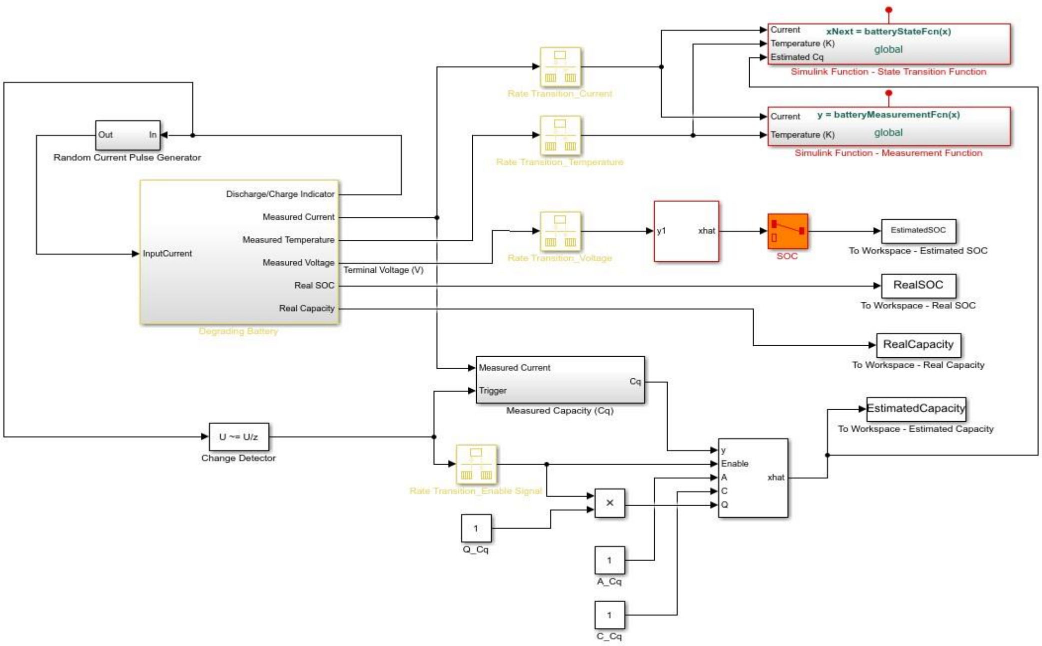

Fig. 3. MATLAB Simulink model of Kalman filtering based SOC Estimation [65]

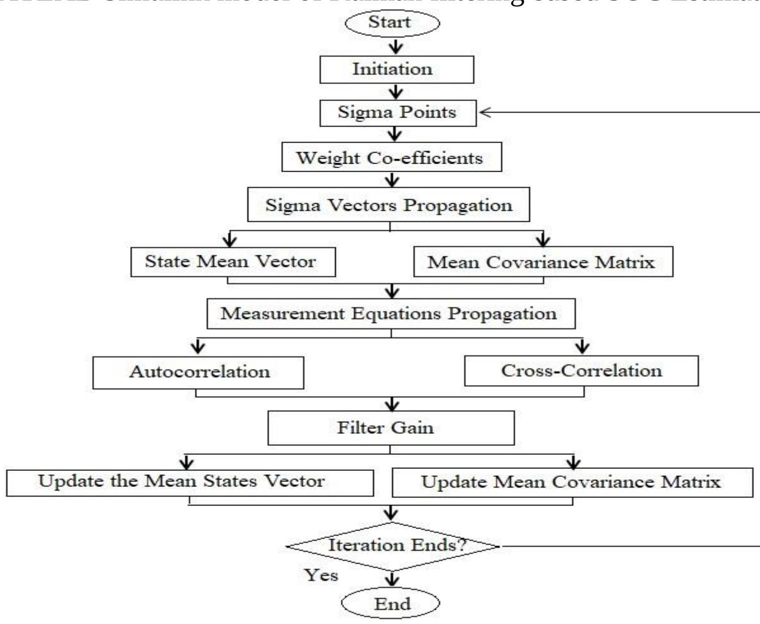

Fig. 4. Flowchart for the implementation of KF based method

The MATLAB Simulink model for the extended Kalman filter is represented in Figure 3. The flowchart for implementation of the proposed Kalman filtering based method, is given in Figure 4.

3. Kalman filters implementation

To forecast the state of a physical or actual process, the KF is based on a set of differential equations (a model). As a result, by adjusting the state variables, it minimises the error between a linear system's measured and expected output. The filter is frequently used in the battery field to forecast cell voltage using an ECM and a coulomb counting. The relationship between the SOC and the OCV is taken into consideration for this reason. The discrepancy between the estimated and measured voltages is then compared, and by modifying the SOC and other ECM variables, it is made as small as possible. State estimation for linear systems can be accomplished using a linear Kalman filter [66, 67].

The linear Kalman filter (LKF) is not frequently utilised in literature because of the non-linear cell behaviour. The KF can be used with batteries using first-order Taylor approximation of the differential equations to linearize the system and measurement matrices in the actual state. Extended Kalman Filter (EKF) is the name of this strategy [68–78]. However, because of the linearization error and the neglect of the higher-order derivatives of the Taylor approximation, filter estimation can lead to erroneous behaviour and divergence of the filter [78]. The sigma point Kalman filter (SPKF) was created for this purpose. Here, a set of sigma points are used to approximate the linearization without the need for derivatives [78-80]. The unscented Kalman filter (UKF) and the central difference Kalman filter (CDKF) are two popular varieties of the SPKF.

An UKF based on the unscented transformation is provided in [67,70,81-85]. By skipping the creation of the system and measurement matrices, this transformation can be used to approximatively determine the desired values and the covariance of a random variables propagated through a nonlinear function [78]. The interpolation used by Stirling provides the foundation for the CDKF [78,8687]. The derivation is omitted, just like in the case of the UKF. The application of scaling and gain factors is related to the distinction between the two filters. The UKF employs three scaling factors, compared to just one in the CDKF.

Both filters drawback is that each time step's square root calculation of the covariance matrix using the Cholesky factorization is necessary. The positive definition of the covariance matrix cannot be guaranteed, and rounding errors can happen. Paper [78,82], introduced the square root forms of the UKF and CDKF to minimize calculation error. The Cholesky factorization is not calculated in each time step but is just updated in this case. Adaptive EKF (AEKF) were developed for decreasing the time for tuning of filters[88-94]. In this, the difference between the actual and anticipated output voltage is used to calculate the process and measurement noise online.

3.a. Kalman filter

Noise is added to the state-space notation in the discrete ECM to account for model and measurement uncertainty. The process noise and measurement noise are represented respectively by the two random variables $wk \in \mathrm{R}n$ and $vk \in \mathrm{R}m$. With this notation, the measurement equation and the state-space representation are expanded to:

$$x_{k+1} = A_k x_k + B_k u_k + w_k \tag{27}$$

$$y_k = H_k x_k + D_k u_k + v_k \tag{28}$$

If the mean values are zero and the measurement noise and process noise are uncorrelated, it may be assumed that:

$$E[ww^t] = \mathrm{Q} \tag{29}$$

$$E[vv^t] = \mathrm{r} \tag{30}$$

As a result, E is the statistical expectation operator, r is the measurement noise covariance and Q is the process noise matrix covariance [95].

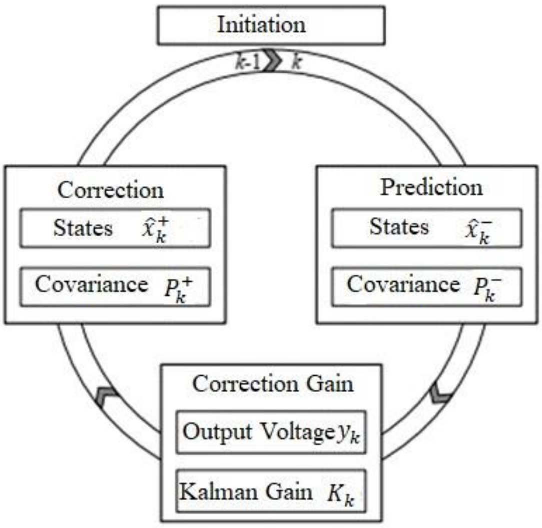

Fig. 5. Calculation sequence of a Kalman filter

Considering certain assumptions, the algorithm simplifies to the following calculation sequence.
Initializing

$$\hat{x}_0^+ = E[x_0] \tag{31}$$

$$P_0^+ = E[(x_0 - \hat{x}_0^+)(x_0 - \hat{x}_0^+)^t] \tag{32}$$

Predicting

$$\hat{x}_k^- = A_{k-1}\hat{x}_{k-1}^+ + B_{k-1}u_{k-1} \tag{33}$$

$$P_k^- = A_{k-1}P_{k-1}^+A_{k-1}^t + Q \tag{34}$$

Correcting gain

$$y_k = H_k\hat{x}_k^- + D_k u_k \tag{35}$$

$$K_k = P_k^- H_k^t(H_k P_k^- H_k^t + r)^{-1} \tag{36}$$

After correcting

$$\hat{x}_k^+ = \hat{x}_k^- - K_k(U_k - y_k) \tag{37}$$

$$P_k^+ = (I - K_k H_k)P_k^- \tag{38}$$

This kind of Kalman filter is referred to as a linear Kalman filter (LKF), in the work that follows. All varieties of Kalman filters use the given calculation process.

3.b. Extended Kalman filter

The state-space equation and measurement equation are taken to have the following forms in order to account for nonlinear behaviour:

$$x_{k+1} = f(x_k, u_k) + w_k \tag{39}$$

$$y_k = e(x_k, u_k) + v_k \tag{40}$$

Given *f* and *e* are two differentiable functions. The first order Taylor expansion can be used to approximate these two functions if their time deviation is minimal. Additionally, either *x*ˆ+ *k* or *x*ˆ- *k*, depending on the most recent state approximation, is used to evaluate the functions. This process makes a distinction between the LKF and the EKF. These presumptions allow the matrices A and H from Equations 27 and 28 to be re-written in the form:

$$A_k = \frac{\partial f(x_k,u_k)}{\partial x_k}|_{x_k} \tag{41}$$

$$H_k = \frac{\partial e(x_k,u_k)}{\partial x_k}|_{x_k} \tag{42}$$

The equations 41 and 42 are often referred to as Jacobian matrices. The extended Kalman filter method functions analogous to the linear Kalman filter when these variances are taken into consideration.

3.c. Adaptive Extended Kalman filter

It is possible to apply the KF to non-linear systems because of the EKF. There are some systems, though, whose dynamical processes and parameters cannot be precisely identified. The KF then makes inaccurate estimations as a result.

The measurement noise and the process noise can utilise the system's remaining degrees of freedom to find a solution to this issue. An accurate estimation of the condition and a quick transient response are produced by selecting these values properly [88,89,96]. The process noise and the measurement noise can also change in each time step as a result of fluctuating environmental effects (like temperature), which affect the approximation [76]. In place of using the measurements noise values, which takes average of overall potential states of the random variables, the concept is to utilise the average values of deviation of measured and anticipated measurements values at the most recent time step. Despite the fact that this goes against the Kalman gain's ability to minimise, the KF replacement takes into account the system's actual behaviour. Calculating the moving average $V\varphi$ of the measurement deviation can be used to put this into practise:

$$V_k^{\emptyset} = \frac{1}{\emptyset}\sum_{m=k-\emptyset+1}^{k}(U_k - y_k)\,(U_k - y_k)^t \tag{43}$$

Using window sizes of $\varphi \leq k$ and $\varphi \in$N. The measurements noise and the process noise matrix are updated as follows [88,89,96] based on the averaged error.

$$r_k = V_k^{\emptyset} + H_k P_k^{-} H_k^t \tag{44}$$

$$Q_k = K_k V_k^{\emptyset} K_k^t \tag{45}$$

3.d. Unscented Kalman filter/ Sigma point Kalman filter

Neither a linear nor a Gaussian distributed system is possible. Additionally, the impact of the noise may not always be linear. As a result, the measurement equation and the state-space equation are

$$x_{k+1} = f(x_k, u_k, w_k) \tag{46}$$

$$y_k = e(x_k, u_k, v_k) \tag{47}$$

The random variable is approximated by other vectors using the differentiable functions f and e, where the covariance matrix and mean value are created so that they are equivalent to the state parameters. The choice of these vectors is unrestricted because both the weights and the number of each sigma point are arbitrary. The probability distribution that was created, though, is simply a rough approximation of the Gaussian distribution. As a result, only in the first two moments of a Taylor approximation are the mean value and covariance matrix equivalent. All odd moments are zero, which is equivalent to the Gaussian distribution. Apart from the Gaussian distribution approximation, the UKF algorithm is identical to all other KFs. Given the process noise, it is necessary to determine 2n+1 sigma points λ_n, where n is the state vector's length. The estimation of the following state can therefore be obtained using the state space in Eq. (46). The measurement equation and covariance matrices are then computed. The derivation and the entire algorithm are described in [78,80,81].

4. Simulation Results and Analysis

The estimation for SOC was carried out using extended Kalman filtering, adaptive extended Kalman filtering and unscented Kalman filtering. For this input measured data contains time, voltage, current and temperature. The simulation results obtained are given in below Figures 6-13.

At first the estimation using extended Kalman filtering was attempted. The Figure 6, shows the measured and estimated battery SOC using extended Kalman filter. The nominal capacity for the battery under investigation is 4.81Ah. It was observed that the battery terminal voltage decreased from 4.2V to 3.73V in 4 hours duration.

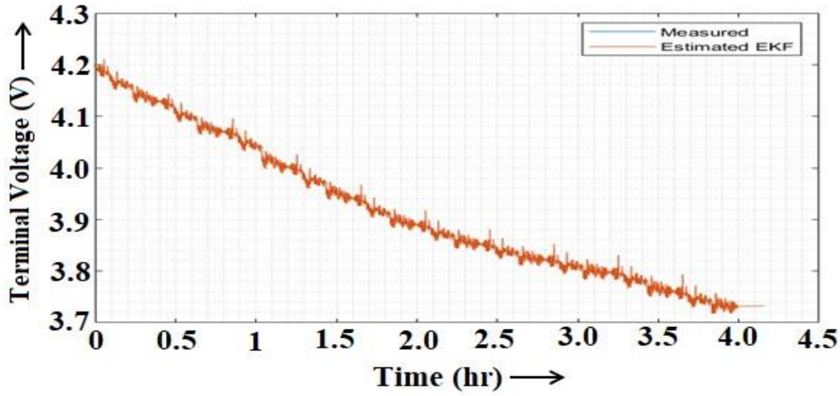

Fig. 6. Actual and estimated Terminal voltage based on EKF vs time plot

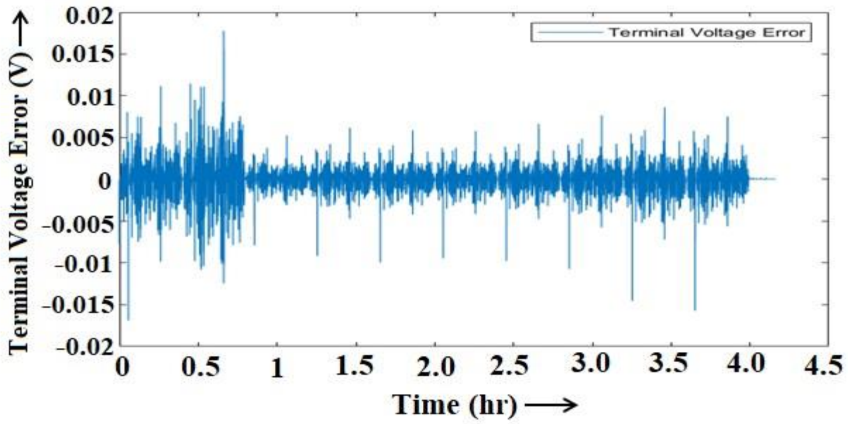

Fig. 7. Terminal voltage error based on EKF vs time plot

The battery terminal voltage error is represented in Figure 7. It was observed that the terminal voltage error is within 0.02V range. The RMSE (root mean square error) value for the battery terminal voltage is 1.31%.

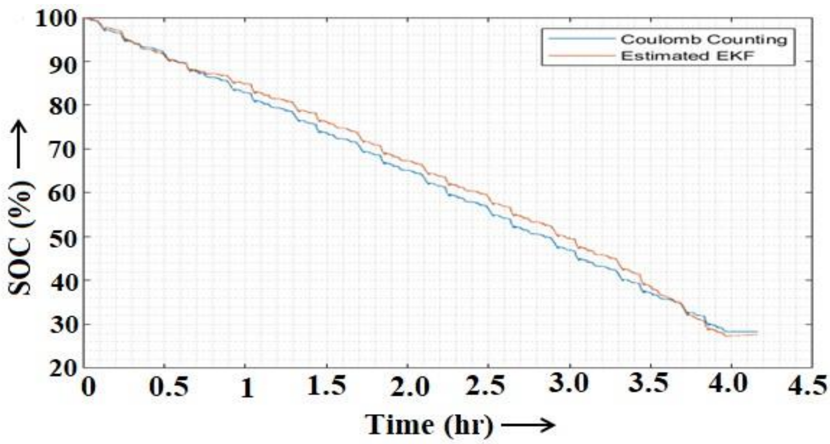

Fig. 8. Coulomb counting and estimated SOC (%) based on EKF vs time plot

The Actual SOC (theoretically calculated using coulomb counting) and SOC estimated using EKF method is shown in Figure 8. It can be seen that the actual and estimated SOC is almost matching. The difference in actual and estimated SOC is also studied. The error is SOC estimation is shown in Figure 9. The root mean square error (RMSE) value for SOC estimation is 1.94%. Maximum error is SOC estimation was observed as 2.80%.

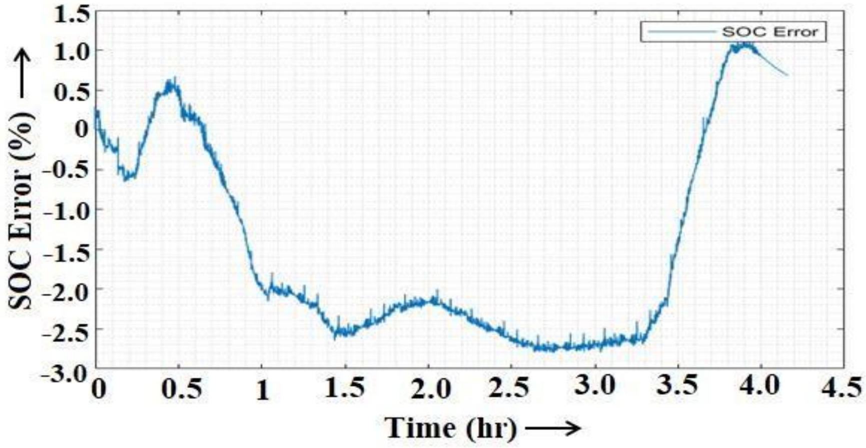

Fig. 9. EKF Based Estimated SOC Error (%) vs time plot

Secondly, adaptive extended Kalman filter (AEKF) based method was used to estimate the SOC of the battery. In AEKF method an additional Kalman gain is included in comparison to EKF method. AEKF method initially gives more error in comparison to EKF method. However, after few minutes it gives better result for the SOC estimation. Figure 10 shows the estimated actual and estimated SOC after 0.5 hours. The estimated SOC error value was also calculated and shown in Figure 11. The RMSE value for SOC Error using AEKF for entire interval was 4.98%. However, it can be seen in the Figure 11 that, maximum SOC error after 0.5 hours interval was within 0.65%.

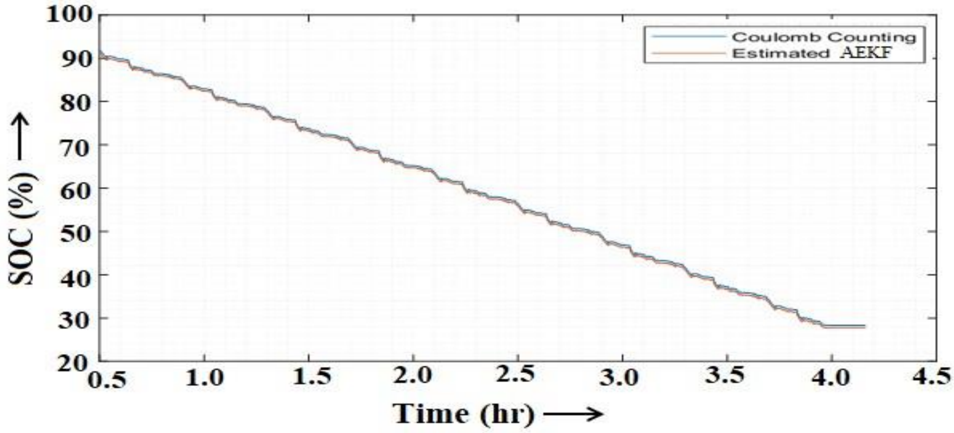

Fig. 10. Actual and Estimated SOC (%) based on AEKF vs time plot

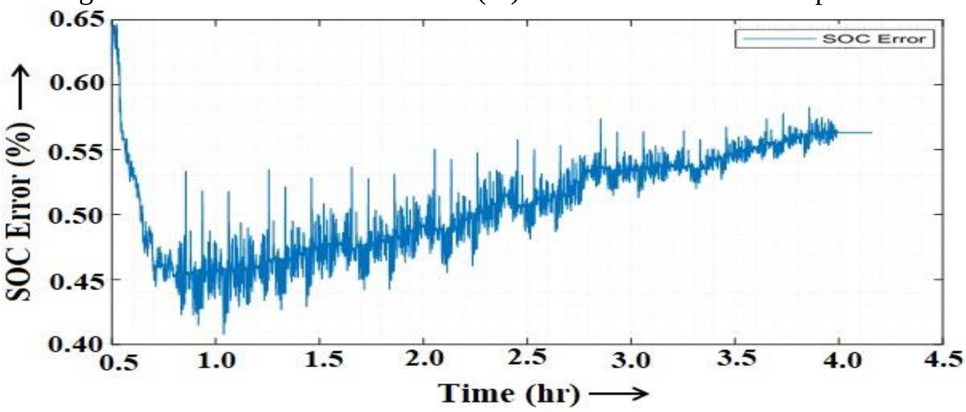

Fig. 11. Estimated SOC error based on AEKF (%) vs time plot

Thirdly, unscented Kalman filter (UKF) based method was used to estimate the SOC of the battery. This gives comparatively better results than the previous two methods. This simulation was run for greater time interval i.e. multiple charge and discharge cycles and it gave satisfactory performance. The actual and estimated SOC based on UKF method is shown in Figure 12.

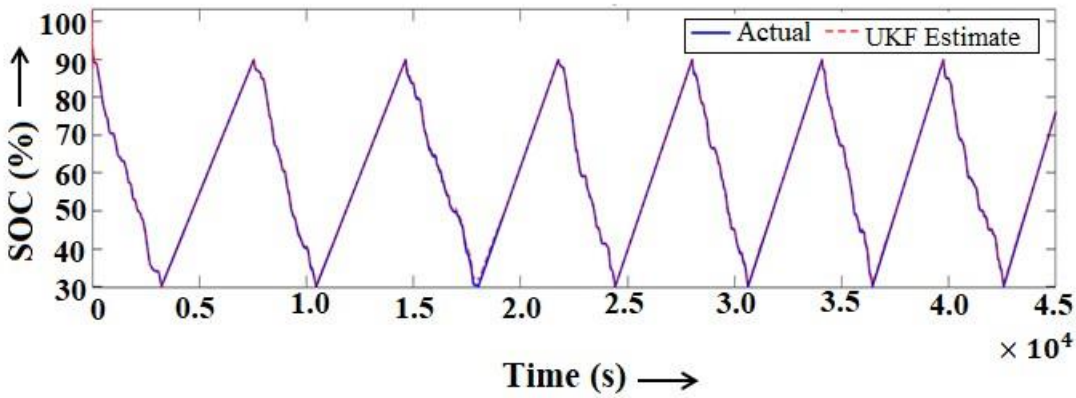

Fig. 12. Actual and estimated SOC based on UKF (%) vs time plot

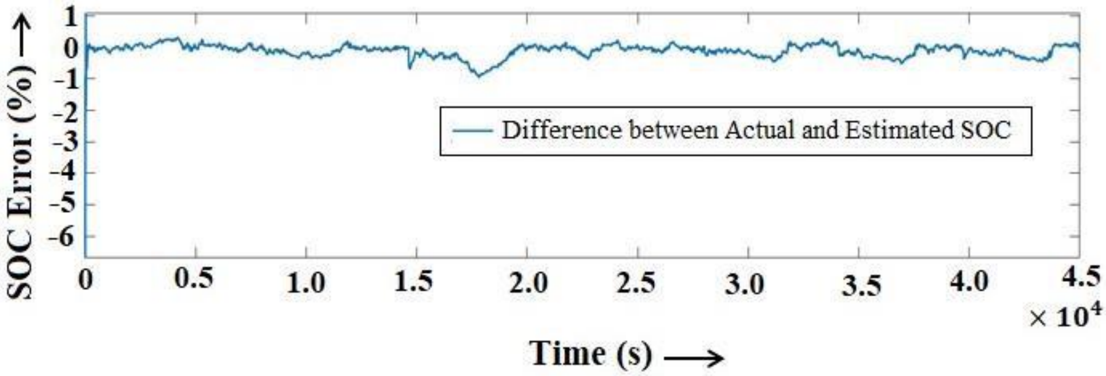

Fig. 13. Actual and estimated based on UKF SOC (%) vs time plot

The difference between the actual SOC and SOC estimated using UKF method is shown in Figure 13. The above result shows that the error is in the range of less than 1%. The best result was obtained in UKF method by tuning the covariance matrices. The best result obtained using this method has RMSE value for SOC Estimation as 0.10%. Maximum SOC error was observed as 0.51%. Hence, it can be said that the UKF gives better estimate for SOC than EKF and AEKF.

5. Conclusion

In this paper, different Kalman filters have been used for the state of charge estimation of the Li-ion battery. These algorithms have been implemented is simulation and the estimation results are compared. Kalman filtering results were compared with experimental data as well. The measurement data and all Kalman filtering methods obtained result had good agreement (less than 5% error), showing that the suggested approaches may accurately predict the SOC of the battery in dynamic situations.The simulation results show that the SOC estimation accuracy of UKF is better than the other KF methods i.e. EKF and AEKF.The simulation result of UKF shows anerror of less than 0.51%.Authors suggest that UKF based methods can be adopted for SOC estimation in battery management system of Li-ion batteries.

References

[1] S. Pang, et al., Interconnection and damping assignment passivity-based control applied to onboard DC–DC power converter system supplying constant power load, IEEE Trans. Ind. Appl. 55 (6) (2019) 6476–6485, http://dx.doi.org/10.1109/TIA.2019.2938149.

[2] Zubi, G.; Dufo-López, R.; Pardo, N.; Pasaoglu, G. Concept development and techno-economic assessment for a solar home system using lithium-ion battery for developing regions to provide electricity for lighting and electronic devices. Energy Convers. Manag. 2016, 122, 439–448.
[3] Y. Liu, R. Ma, S. Pang, L. Xu, D. Zhao, J. Wei, Y. Huangfu, F. Gao, A nonlinear observer SOC estimation method based on electrochemical model for lithium-ion battery, IEEE Trans. Ind. Appl. 57 (2021) 1094–1104, http://dx.doi.org/10.1109/tia.2020.3040140.
[4] Z. Wei, C. Zou, F. Leng, B.H. Soong, K. Tseng, Online model identification and state-of-charge estimate for lithium-ion battery with a recursive total least squares-based observer, IEEE Trans. Ind. Electron. 65 (2) (2018) 1336–1346, http://dx.doi.org/10.1109/TIE.2017.2736480.
[5] C. Zhang, L.Y. Wang, X. Li, W. Chen, G.G. Yin, J. Jiang, Robust and adaptive estimation of state of charge for lithium-ion batteries, IEEE Trans. Ind. Electron. 62 (8) (2015) 4948–4957, http://dx.doi.org/10.1109/TIE.2015.2403796.
[6] Ng KS, Moo CS, Chen YP, et al. (2008) State-of-charge estimation for lead-acid batteries based on dynamic open-circuit voltage. Power and Energy Conference, 2008. PE Con 2008. IEEE 2nd International 972–976.
[7] Xiong R, Cao J, Yu Q, et al. (2018) Critical review on the battery state of charge estimation methods for electric vehicles. Ieee Access 6: 1832–1843.
[8] Ren H, Zhao Y, Chen S, et al. (2019) Design and implementation of a battery management system with active charge balance based on the soc and soh online estimation. Energy 166: 908–917.
[9] Satadru D, Beshah A, Pierluigi P (2015) Nonlinear robust observers for state-of-charge estimation of lithium-ion cells based on a reduced electrochemical model. IEEE Trans Control Syst Technol 23: 1935–1942.
[10] Tang X, Liu B, Gao F (2017) State of charge estimation of lifepo4 battery based on a gainclassifier observer. Energy Procedia 105: 2071–2076.
[11] M. Kwak, B. Lkhagvasuren, J. Park, J. You, Parameter identification and SOC estimation of a battery under the hysteresis effect, IEEE Trans. Ind. Electron. 67 (11) (2020) 9758–9767, http://dx.doi.org/10.1109/TIE.2019.2956394.
[12] S. Afshar, K. Morris, A. Khajepour, State-of-charge estimation using an EKF-based adaptive observer, IEEE Trans. Control Syst. Technol. 27 (5) (2019) 1907–1923, http://dx.doi.org/10.1109/TCST.2018.2842038.
[13] Q. Wang, J. Kang, Z. Tan, M. Luo, An online method to simultaneously identify the parameters and estimate states for lithium ion batteries, Electrochim. Acta 289 (2018) 376–388, http://dx.doi.org/10.1016/j.electacta.2018.08.076.
[14] Bo Yang, Junting Wang, Pulin Cao, Tianjiao Zhu, Hongchun Shu, Jiao Chen, Jin Zhang, Jiawei Zhu, Classification, summarization and perspectives on state-of-charge estimation of lithium-ion batteries used in electric vehicles: A critical comprehensive survey, J. Energy Storage 39 (2021) 102572, http://dx.doi.org/10.1016/j.est.2021.102572.
[15] F. Sanchez Gorostiza, F.M. Gonzalez-Longatt, Deep reinforcement learning-based controller for SOC management of multi-electrical energy storage system, IEEE Trans. Smart Grid 11 (6) (2020) 5039–5050, http://dx.doi.org/10.1109/TSG.2020.2996274.
[16] Guozhou Zhang, Weihao Hu, Di Cao, Qi Huang, Jianbo Yi, Zhe Chen, FredeBlaabjerg, Deep reinforcement learning based approach for proportional resonance power system stabilizer to prevent ultra-low-frequency oscillations, IEEE Trans. Smart Grid 11 (6) (2020) 5260–5272, http://dx.doi.org/10.1109/TSG.2020.2997790.
[17] Guozhou Zhang, Weihao Hu, Di Cao, Wen Liu, Rui Huang, Qi Huang, Zhe Chen, FredeBlaabjerg, Data-driven optimal energy management for a wind-solar-diesel-battery-reverse osmosis hybrid energy system using a deep reinforcement learning approach, Energy Convers. Manage. 227 (2021) 113608, http://dx.doi.org/10.1016/j.enconman.2020.113608.

[18] D. Cao, et al., Reinforcement learning and its applications in modern power and energy systems: A review, J. Mod. Power Syst. Clean Energy 8 (6) (2020) 1029–1042, http://dx.doi.org/10.35833/MPCE.2020.000552.
[19] Rezaei, O.; Alinejad, M.; Nejati, S.A.; Chong, B. An optimized adaptive estimation of state of charge for Lithium-ion battery based on sliding mode observer for electric vehicle application. In Proceedings of the 2020 8th International Conference on Intelligent and Advanced Systems (ICIAS), Kuching, Malaysia, 13–15 July 2021; pp. 1–6.
[20] M. Shehab El Din, A.A. Hussein, M.F. Abdel-Hafez, Improved battery SOC estimation accuracy using a modified UKF with an adaptive cell model under real EV operating conditions, IEEE Trans TranspElectrif 4 (2) (2018) 408–417, http://dx.doi.org/10.1109/TTE.2018.2802043.
[21] Pei, L.; Lu, R.; Zhu, C. Relaxation model of the open-circuit voltage for state-of-charge estimation in lithium-ion batteries. IET Electr. Syst. Transp. 2013, 3, 112–117.
[22] Cheng, M.W.; Lee, Y.S.; Liu, M.; Sun, C.C. State-of-charge estimation with aging effect and correction for lithium-ion battery. IET Electr. Syst. Transp. 2015, 5, 70–76.
[23] N. Watrin, B. Blunier, A. Miraoui, Transportation Electrification Conference and Expo (ITEC), 2012 IEEE, pp.1-6, 18-20 June 2012.
[24] Gholizadeh, M.; Yazdizadeh, A. State of charge estimation of a lithium-ion battery using robust nonlinear observer approach. IET Electr. Syst. Transp. 2018, 9, 1–7.
[25] Zhang, Z.; Zhou, D.; Xiong, N.; Zhu, Q. Non-fragile H¥ nonlinear observer for state of charge estimation of lithium-ion battery based on a fractional-order model. Energies 2021, 14, 4771.
[26] Ebrahimi, F.; Abedi, M. Design of a robust central difference Kalman filter in the presence of uncertainties and unknown measurement errors. Signal Process. 2020, 172, 107533.
[27] Chen, N.; Zhang, P.; Dai, J.; Gui, W. Estimating the state-of-charge of lithium-ion battery using an H-infinity observer based on electrochemical impedance model. IEEE Access 2020, 8, 26872– 26884.
[28] Verbrugge, M.; Tate, E. Adaptive state of charge algorithm for nickel metal hydride batteries including hysteresis phenomena. J. Power Sources 2004, 126, 236–249.
[29] Chen, Z.; Sun, H.; Dong, G.; Wei, J.; Wu, J.I. Particle filter-based state-of-charge estimation and remaining-dischargeable-time prediction method for lithium ion batteries. J. Power Source 2019, 414, 158–166.
[30] Xia, B.; Chen, C.; Tian, Y.; Sun, W.; Xu, Z.; Zheng, W. A novel method for state of charge estimation of lithium-ion batteries using a nonlinear observer. J. Power Sources 2014, 270, 359–366.
[31] Hu, Y.; Yurkovich, S. Battery cell state-of-charge estimation using linear parameter varying system techniques. J. Power Sources 2012, 198, 338–350.
[32] Gholizadeh, M.; Salmasi, F.R. Estimation of state of charge, unknown nonlinearities, and state of health of a lithium-ion battery based on a comprehensive unobservable model. IEEE Trans. Ind. Electron. 2013, 61, 1335–1344.
[33] Rezaei, O.; Moghaddam, H.A.; Papari, B. A fast sliding-mode-based estimation of state-of charge for lithium-ion batteries for electric vehicle applications. J. Energy Storage 2022, 45, 103484.
[34] Chen, X.; Shen, W.; Cao, Z.; Kapoor, A. A novel approach for state of charge estimation based on adaptive switching gain sliding mode observer in electric vehicles. J. Power Sources 2014, 246, 667–678.
[35] Chan, C.C.; Lo, E.W.C.; Shen, W. The available capacity computation model based on artificial neural network for lead–acid batteries in electric vehicles. J. Power Sources 2000, 87, 201–204.
[36] Shen, W.X.; Chan, C.C.; Lo, E.W.C.; Chau, K.T. A new battery available capacity indicator for electric vehicles using neural network. Energy Convers. Manag. 2002, 43, 817–826.
[37] Yang, F.; Li, W.; Li, C.; Miao, Q. State-of-charge estimation of lithium-ion batteries based on gated recurrent neural network. Energy 2019, 175, 66–75.
[38] Habibifar, R.; Karimi, M.R.; Ranjbar, H.; Ehsan, M. Economically based distributed battery energy storage systems planning in microgrids. In Proceedings of the Iranian Conference on Electrical Engineering (ICEE), Mashhad, Iran, 8–10 May 2018; pp. 1257–1263.

[39] Charkhgard, M.; Farrokhi, M. State-of-charge estimation for lithium-ion batteries using neural networks and EKF. IEEE Trans. Ind. Electron. 2010, 57, 4178–4187.
[40] Xu, P.; Liu, B.; Hu, X.; Ouyang, T.; Chen, N. State-of-charge estimation for lithium-ion batteries based on fuzzy information granulation and asymmetric Gaussian membership function. IEEE Trans. Ind. Electron. 2021, 69, 6635–6644.
[41] Huang, Z.; Fang, Y.; Xu, J. SoC estimation of li-ion battery based on improved EKF algorithm. Int. J. Automot. Technol. 2021, 22, 335–340.
[42] Hannan, M.A.; How, D.N.; Lipu, M.S.; Mansor, M.; Ker, P.J.; Dong, Z.Y.; Sahari, K.S.M.; Tiong, S.K.; Muttaqi, K.M.; Mahlia, T.M.; et al. Deep learning approach towards accurate state of charge estimation for lithium-ion batteries using self-supervised transformer model. Sci. Rep. 2021, 11, 1–13.
[43] Lipu, M.S.H.; Hannan, M.A.; Hussain, A.; Saad, M.H.; Ayob, A.; Uddin, M.N. Extreme learning machine model for state-of-charge estimation of lithium-ion battery using gravitational search algorithm. IEEE Trans. Ind. Appl. 2019, 55, 4225–4234.
[44] Bian, C.; Yang, S.; Miao, Q. Cross-domain state-of-charge estimation of Li-ion batteries based on deep transfer neural network with multiscale distribution adaptation. IEEE Trans. Transp. Electrif. 2020, 7, 1260–1270.
[45] Ng, K.S.; Moo, C.; Chen, Y.; Hsieh, Y. Enhanced coulomb counting method for estimating stateof-charge and state-of-health of lithium-ion batteries. Appl. Energy 2009, 86, 1506–1511, doi:10.1016/j.apenergy.2008.11.021.
[46] W. He, N. Williard, C. Chen, M. Pecht, Microelectronic Reliability (2013). Available online at: http://dx.doi.org/10.1016/j.microrel.2012.11.010.
[47] Jeong, Y.M. Enhanced coulomb counting method with adaptive SOC reset time for estimating OCV. In IEEE Energy Conversion Congress and Exposition ECCE, Proceedings of the 2014 Energy Conversion Congress and Exposition, Pittsburgh, PA, USA, 14–18 September 2014; IEEE: New York, NY, USA, 2014; pp. 4313–4318.
[48] Yu, Z.; Huai, R.; Xiao, L. State-of-charge estimation for lithium-ion batteries using a Kalman filter based on local linearization. Energies 2015, 8, 7854–7873.
[49] He, H. State-of-charge estimation of the lithium-ion battery using an adaptive extended Kalman filter based on an improved Thevenin model. IEEE Trans. Veh. Technol. 2011, 60, 1461–1469.
[50] Li, W.; Yang, Y.; Wang, D.; Yin, S. The multi-innovation extended Kalman filter algorithm for battery SOC estimation. Ionics 2020, 26, 6145–6156.
[51] Malysz, P.; Gu, R.; Ye, J.; Yang, H.; Emadi, A. State-of-charge and state-of-health estimation with state constraints and current sensor bias correction for electrified powertrain vehicle batteries. IET Electr. Syst. Transp. 2016, 6, 136–144.
[52] Gholizadeh, M.; Yazdizadeh, A. Systematic mixed adaptive observer and EKF approach to estimate SOC and SOH of lithium–ion battery. IET Electr. Syst. Transp. 2019, 10, 135–143.
[53] Kim, J.; Cho, B.H. State-of-charge estimation and state-of-health prediction of a Li-ion degraded battery based on an EKF combined with a per-unit system. IEEE Trans. Veh. Technol. 2011, 60, 4249–4260.
[54] Chen, Z.; Fu, Y.; Mi, C.C. State of charge estimation of lithium-ion batteries in electric drive vehicles using extended Kalman filtering. IEEE Trans. Veh. Technol 2013, 62, 1020–1030.
[55] Li, J.; Ye, M.; Gao, K.; Jiao, S.; Xu, X. A novel battery state estimation model based on unscented Kalman filter. Ionics 2021, 27, 2673–2683.
[56] Sun, F.; Hu, X.; Zou, Y.; Li, S. Adaptive unscented Kalman filtering for state of charge estimation of a lithium-ion battery for electric vehicles. Energy 2011, 36, 3531–3540.
[57] Plett, G. Sigma-point Kalman filtering for battery management systems of LIPB-based HEV battery packs: Part 2: Simultaneous state and parameter estimation. J. Power Source 2006, 161, 1369– 1384.

[58] Sangwan, V.; Kumar, R.; Rathore, A.K. State-of-charge estimation for Li-ion battery using extended Kalman filter (EKF) and central difference Kalman filter (CDKF). In Proceedings of the 2017 IEEE Industry Applications Society Annual Meeting, Cincinnati, OH, USA, 1–5 October 2017; pp. 1–6.
[59] Chen, D.; Wang, C.; Zhu, Z.; Zou, Z. Lithium battery state-of-charge estimation based on interactive multi-model unscented Kalman filter Algorithm. Energy Storage Sci. Technol. 2020, 9, 257.
[60] V.H. Johnson, Battery performance models in ADVISOR, J Power Sources 110 (2002) 321–329, http://dx.doi.org/10.1016/S0378-7753(02)00194-5.
[61] J. Kim, B.H. Cho, State-of-charge estimation and state-of-health prediction of a li-ion degraded battery based on an EKF combined with a per-unit system, IEEE Trans. Veh. Technol. 60 (9) (2011) 4249–4260, http://dx.doi.org/10.1109/TVT.2011.2168987.
[62] Z. Chen, Y. Fu, C.C. Mi, State of charge estimation of lithium-ion batteries in electric drive vehicles using extended Kalman filtering, IEEE Trans. Veh. Technol. 62 (3) (2013) 1020–1030, http://dx.doi.org/10.1109/TVT.2012.2235474.
[63] Chen, M.; Rincon-Mora, G.A. Accurate electrical battery model capable of predicting runtime and IV performance. IEEE Trans. Energy Convers. 2006, 21, 504–511.
[64] G. Plett, J. Power Sources 134 (2004) 262-276.
[65] I.U Khalil, Matiullah Ahsan, Irshad Ullah, Arbab Adnan, Naveed Khan, Shah Nawaz, SOC prediction of Lithium-Ion Battery using Extended Kalman Filter, IEEE Xplore.
[66] K. Lim, H. A. Bastawrous, V.-H. Duong, K. W. See, P. Zhang, and S. X. Dou. “Fading Kalman filter-based real-time state of charge estimation in LiFePO4 battery-powered electric vehicles”. In: Appl. Energy. 169 (2016), pp. 40–48. doi: 10.1016/j.apenergy.2016.01.096.
[67] D. Andre, C. Appel, T. Soczka-Guth, and D. U. Sauer. “Advanced mathematical methods of SOC and SOH estimation for lithium-ion batteries”. In: J. Power Sources 224 (2013), pp. 20–27. doi: 10.1016/j.jpowsour.2012.10.001.
[68] G. L. Plett. “Extended Kalman filtering for battery management systems of LiPBbased HEV battery packs Part 3. State and parameter estimation”. In: J. Power Sources 134.2 (2004), pp. 277– 292. doi: 10.1016/j.jpowsour.2004.02.033.
[69] P. Zarchan and H. Musoff. Fundamentals of Kalman filtering: A practical approach. 3rd ed. Vol. 232. Progress in astronautics and aeronautics. Reston and Va: American Institute of Aeronautics and Astronautics, 2009.
[70] Y. He, X. Liu, C. Zhang, and Z. Chen. “A new model for State-of-Charge (SOC) estimation for high-power Li-ion batteries”. In: Appl. Energy. 101 (2013), pp. 808–814. doi: 10.1016/j.apenergy.2012.08.031.
[71] J. Lee, O. Nam, and B. H. Cho. “Li-ion battery SOC estimation method based on the reduced order extended Kalman filtering”. In: J. Power Sources 174.1 (2007), pp. 9–15. doi: 10.1016/j.jpowsour.2007.03.072.
[72] S. Lee, J. Kim, J. Lee, and B. H. Cho. “State-of-charge and capacity estimation of lithium-ion battery using a new open-circuit voltage versus state-of-charge”. In: J. Power Sources 185.2 (2008), pp. 1367–1373. doi: 10.1016/j.jpowsour.2008.08.103.
[73] J. Kim and B. H. Cho. “State-of-Charge Estimation and State-of-Health Prediction of a Li-Ion Degraded Battery Based on an EKF Combined With a Per-Unit System”. In: IEEE T VehTechnol 60.9 (2011), pp. 4249–4260. doi: 10.1109/TVT.2011.2168987.
[74] H. He, H. Qin, X. Sun, and Y. Shui. “Comparison Study on the Battery SoC Estimation with EKF and UKF Algorithms”. In: Energies 6.10 (2013), pp. 5088–5100. doi: 10.3390/en6105088.
[75] J. T. B. A. Kessels, B. Rosca, H. J. Bergveld, and van den Bosch,P. P. J. “On-line battery identification for electric driving range prediction”. In: Vehicle Power and Propulsion Conference (2011), pp. 1–6. doi: 10.1109/VPPC.2011.6043022.

[76] C. Zhang, J. Jiang, W. Zhang, and S. M. Sharkh. "Estimation of State of Charge of Lithium-Ion Batteries Used in HEV Using Robust Extended Kalman Filtering". In: Energies 5.12 (2012), pp. 1098–1115. doi: 10.3390/en5041098.
[77] J. Li, J. Klee Barillas, C. Guenther, and M. A. Danzer. "A comparative study of state of charge estimation algorithms for LiFePO4 batteries used in electric vehicles". In: J. Power Sources 230 (2013), pp. 244–250. doi: 10.1016/j.jpowsour.2012.12.057.
[78] Rudolph van der Merwe. "Sigma-Point Kalman Filters for Probabilistic Inference in Dynamic State-Space Models". PhD thesis. Oregon: Oregon Health & Science University, 2004.
[79] G. L. Plett. "Sigma-point Kalman filtering for battery management systems of LiPBbased HEV battery packs Part 2: Simultaneous state and parameter estimation". In: J. Power Sources 161.2 (2006), pp. 1369–1384. doi: 10.1016/j.jpowsour.2006.06.004.
[80] G. L. Plett. "Sigma-point Kalman filtering for battery management systems of LiPB based HEV battery packs Part 1: Introduction and state estimation". In: J. Power Sources 161.2 (2006), pp. 1356– 1368. doi: 10.1016/j.jpowsour.2006.06.003.
[81] H. He, R. Xiong, and J. Peng. "Real-time estimation of battery state-of-charge with unscented Kalman filter and RTOS uCOS-II platform". In: Appl. Energy. (2015). doi: 10.1016/j.apenergy.2015.01.120.
[82] Y. Tian, B. Xia, W. Sun, Z. Xu, and W. Zheng. "A modified model based state of charge estimation of power lithium-ion batteries using unscented Kalman filter". In: J. Power Sources 270 (2014), pp. 619–626. doi: 10.1016/j.jpowsour.2014.07.143.
[83] E. A. Wan and van der Merwe, Rudolph. "The unscented Kalman Filter". In: Kalman filtering and neural networks. Ed. by S. S. Haykin. Adaptive and learning systems for signal processing, communications, and control. New York: Wiley, 2001, pp. 221–280.
[84] Y. Xing, W. He, M. Pecht, and K. L. Tsui. "State of charge estimation of lithium-ion batteries using the open-circuit voltage at various ambient temperatures". In: Appl. Energy. 113 (2014), pp. 106–115. doi: 10.1016/j.apenergy.2013.07.008.
[85] X. Zheng and H. Fang. "An integrated unscented kalman filter and relevance vector regression approach for lithium-ion battery remaining useful life and short-term capacity prediction". In: Rliabengsyst safe 144 (2015), pp. 74–82. doi: 10.1016/j.ress.2015.07.013.
[86] L. Wang, L. Wang, C. Liao, and J. Liu. "Sigma-point Kalman filter application on estimating battery SOC". In: IEEE Vehicle Power and Propulsion Conference (VPPC). 2009, pp. 1592–1595. doi: 10.1109/VPPC.2009.5289604.
[87] J. Remmlinger, M. Buchholz, T. Soczka-Guth, and K. Dietmayer. "On-board state-ofhealth monitoring of lithium-ion batteries using linear parameter-varying models". In: J. Power Sources 239 (2013), pp. 689–695. doi: 10.1016/j.jpowsour.2012.11.102.
[88] J. Han, D. Kim, and M. Sunwoo. "State-of-charge estimation of lead-acid batteries using an adaptive extended Kalman filter". In: J. Power Sources 188.2 (2009), pp. 606–612. doi: 10.1016/j.jpowsour.2008.11.143.
[89] H. He, R. Xiong, and H. Guo. "Online estimation of model parameters and state-ofcharge of LiFePO4 batteries in electric vehicles". In: Appl. Energy. 89.1 (2012), pp. 413–420. doi: 10.1016/j.apenergy.2011.08.005.
[90] R. Xiong, H. He, F. Sun, X. Liu, and Z. Liu. "Model-based state of charge and peak power capability joint estimation of lithium-ion battery in plug-in hybrid electric vehicles". In: J. Power Sources 229 (2013), pp. 159–169. doi: 10.1016/j.jpowsour.2012.12.003.
[91] F. Sun, R. Xiong, and H. He. "Estimation of state-of-charge and state-of-power capability of lithium-ion battery considering varying health conditions". In: J. Power Sources 259 (2014), pp. 166– 176. doi: 10.1016/j.jpowsour.2014.02.095.
[92] H. He, Z. Liu, and Y. Hua. "Adaptive Extended Kalman Filter Based Fault Detection and Isolation for a Lithium-Ion Battery Pack". In: Energy Procedia 75 (2015), pp. 1950–1955. doi:

10.1016/j.egypro.2015.07.230.
[93] Y. Wang, C. Zhang, and Z. Chen. “An adaptive remaining energy prediction approach for lithium-ion batteries in electric vehicles”. In: J. Power Sources 305 (2016), pp. 80–88. doi: 10.1016/j.jpowsour.2015.11.087.
[94] R. Xiong, X. Gong, C. C. Mi, and F. Sun. “A robust state-of-charge estimator for multiple types of lithium-ion batteries using adaptive extended Kalman filter”. In: J. Power Sources 243 (2013), pp. 805–816. doi: 10.1016/j.jpowsour.2013.06.076.
[95] G. L. Plett. “Extended Kalman filtering for battery management systems of LiPB based HEV battery packs Part 1. Background”. In: J. Power Sources 134.2 (2004), pp. 252–261. doi: 10.1016/j.jpowsour.2004.02.031.
[96] R. Xiong, F. Sun, X. Gong, and H. He. “Adaptive state of charge estimator for lithiumion cells series battery pack in electric vehicles”. In: J. Power Sources 242 (2013), pp. 699–713. doi: 10.1016/j.jpowsour.2013.05.071.